

## Insulating spin-glass system $\text{Eu}_x\text{Sr}_{1-x}\text{S}$

H. Maletta

*Institut für Festkörperforschung, Kernforschungsanlage Jülich,  
5170 Jülich, West Germany*

W. Felsch

*I. Physikalisches Institut der Universität,  
3400 Göttingen, West Germany*

(Received 21 September 1978; revised manuscript received 12 March 1979)

A systematic experimental study of the magnetic properties in insulating  $\text{Eu}_x\text{Sr}_{1-x}\text{S}$  is reported, giving evidence of spin-glass behavior for concentrations  $0.13 \leq x \leq 0.5$  due to short-ranged exchange interactions with opposite sign. The magnetic properties below the spin-glass transition temperature  $T_f$  are explored by low-field magnetization, ac susceptibility, and neutron-diffraction measurements. The magnetization and remanent magnetization are found to depend on the thermomagnetic history. An unusually pronounced maximum is observed in the thermoremanent magnetization as function of the previously applied field. The saturation values of the remanent magnetizations remain only a few percent of the saturation magnetizations, even for the high Eu concentrations. Their temperature, field, and time dependence are studied. Comparison is made with metallic spin-glass samples. A detailed experimental study of the susceptibility at the spin-glass transition  $T_f$  in  $(\text{Eu},\text{Sr})\text{S}$  is presented exhibiting a strong sensitivity of  $\chi(T_f)$  and  $T_f$  to small external magnetic fields and different measuring frequencies. In an attempt to analyze the data, the distinction between the spin-glass phenomenon and superparamagnetism is stressed. Near the percolation threshold of the exchange interactions,  $x_p = 0.13$ , a transition from spin-glass behavior to "pure" superparamagnetism is clearly observed in  $\text{Eu}_x\text{Sr}_{1-x}\text{S}$ .

### I. INTRODUCTION

The concept "spin glass" has given rise to a considerable amount of experimental and theoretical work on dilute alloys.<sup>1,2</sup> It is applied to the phenomenon that by lowering the temperature in zero external field the impurity spins "freeze out" or become "locked" in random directions, i.e., the vector average of all local moments gives no net macroscopic moment, and there is no long-range magnetic order. In dilute alloys the local moments are coupled via the conduction electrons by the Ruderman-Kittel-Kasuya-Yosida mechanism (RKKY).<sup>3</sup> This interaction is of long range and an oscillatory function of the distance between the magnetic impurities, resulting in a mixed coupling among the moments in dilute alloys and obviously in this new type of magnetic behavior.

The most prominent feature of a spin glass, the "cusp" in the low-field ac susceptibility at the "freezing temperature"  $T_f$ , first observed in  $\text{AuFe}$  by Cannella and Mydosh,<sup>4</sup> suggests a thermodynamic phase transition at  $T_f$ . On the other hand properties like the rounded maximum in the specific heat or the low temperature ( $T \leq T_f$ ) reversible and irreversible

magnetization with characteristic long-time relaxation effects sometimes are tried to be understood in terms of a Néel model of "superparamagnetic clouds", i.e., some kind of blocking phenomenon leads to non-equilibrium metastable states below  $T_f$ .<sup>5</sup> Also from the theoretical point of view, the nature of the ordering process in spin glasses is presently unresolved,<sup>6</sup> in spite of some success for instance of the Edwards-Anderson model<sup>7</sup> and impressive computer experiments.<sup>8</sup> Even the mathematical treatment of the famous Edwards-Anderson model and its relevance to real systems are a question of some controversy today.

For a better understanding of the spin-glass state, it should be worthwhile, in our opinion, to look for similar properties in other systems than the classical alloys  $\text{AuFe}$  or  $\text{CuMn}$ . In studying the concentration-dependent properties in alloys of transition elements in noble metals, several restrictions for such a model system appear due to metallurgical clustering; the overlap of the direct exchange on the RKKY interaction, or the Kondo effect. Furthermore the question arises whether the RKKY interaction is a necessary condition for spin-glass behavior. Recently, Mydosh<sup>9</sup> has listed and discussed the most recent

spin-glass systems. In his opinion the random insulating materials should not be included into the spin-glass concept since they do not possess the strong RKKY interaction.

Two years ago we performed<sup>10</sup> a Mössbauer study on the insulating system  $\text{Eu}_x\text{Sr}_{1-x}\text{S}$ . EuS orders ferromagnetically below 16.6 K. By dilution with the isostructural, diamagnetic SrS the Curie temperature is lowered steeply near  $x = 0.5$ , indicating a different type of magnetic behavior below this concentration. This is supported by an anomalous temperature and concentration dependence of the Mössbauer spectra characterizing a magnetic inhomogeneous behavior in the low-Eu-concentration regime of  $(\text{Eu},\text{Sr})\text{S}$ , in similarity to spin glasses.

With respect to several aspects, the insulating  $\text{Eu}_x\text{Sr}_{1-x}\text{S}$  system appears as a suitable solid solution series in order to investigate in detail the magnetic ordering behavior for a random system over the whole concentration range  $0 < x \leq 1$ , experimentally as well as theoretically. EuS, a member of the well-studied Eu monochalcogenides, is generally considered as a model substance for Heisenberg ferromagnets.<sup>11</sup> The dilution of EuS with SrS<sup>10</sup> does not change the electronic structure appreciably. The Eu atoms remain in their divalent state characterized by an  $^8S_{7/2}$  ground-state with no significant crystal-field effects; the  $4f$  wave functions are highly localized. In these insulating samples the exchange interactions  $J$  between the Eu moments have been intensively investigated and are generally believed to be restricted to the first- and second-nearest neighbors<sup>12</sup>: the ferromagnetic exchange  $J_1$  to the 12 nearest and the antiferromagnetic exchange  $J_2$  via the anion to the 6 next-nearest Eu neighbors, with  $J_2/J_1 \approx -0.5$  in EuS.

In the present paper we report on further systematic experiments in  $\text{Eu}_x\text{Sr}_{1-x}\text{S}$  confirming spin-glass properties for  $x \leq 0.5$ , in spite of the samples not being metallic. Section III describes the results from ac susceptibility, low-field magnetization, and neutron-diffraction measurements at low temperatures. The spin-glass transition at  $T_f$  is studied in detail by susceptibility measurements as a function of external magnetic field and different measuring frequency. The experiments reveal a low-concentration limit of the spin-glass regime in  $\text{Eu}_x\text{Sr}_{1-x}\text{S}$  at  $x_p = 0.13$ . In Sec. IV, the experimental results are discussed by comparing the observed behavior in  $(\text{Eu},\text{Sr})\text{S}$  to that of a metallic spin-glass system like  $\text{AuFe}$ . The magnetic properties below the spin-glass transition temperature  $T_f$  are studied with emphasis on the reversible and irreversible magnetic properties depending on thermomagnetic effects and on time. Then the nature of the spin-glass transition at  $T_f$  is discussed in view of the measured pronounced field and time effects on the magnetic susceptibility near  $T_f$ . We stress the difference between spin-glass behavior and superparamagnetism in analyzing our experimental

data on  $(\text{Eu},\text{Sr})\text{S}$ . The concentration dependence of several magnetic properties is considered in order to characterize the spin-glass behavior of insulating  $(\text{Eu},\text{Sr})\text{S}$ .

## II. EXPERIMENTAL DETAILS

The  $(\text{Eu},\text{Sr})\text{S}$  samples were prepared chemically via the mixed oxalate of  $\text{Eu}^{3+}$  and  $\text{Sr}^{2+}$ . They were placed into a horizontal quartz tube and treated with a stream of pure  $\text{H}_2\text{S}$  at a temperature of 900 C for five hours. After this time the mixed sulfides had formed. By x-ray analysis they proved to be single phase with the NaCl structure. The lattice constant changes linearly with concentration, with a total amount of only 1% over the whole solid solution series. We have investigated eight powder samples of  $\text{Eu}_x\text{Sr}_{1-x}\text{S}$  with  $x = 0.05, 0.10, 0.15, 0.20, 0.25, 0.30, 0.40$ , and  $0.50$ .

The low-field ( $\approx 10^{-5}$  T), low-frequency (117 Hz) differential magnetic susceptibility,  $ac-\chi$ , was measured for temperatures between 70 mK and 10 K, using a conventional mutual inductance method. The magnetic field dependence of  $ac-\chi$  was investigated by superposing a static magnetic field up to 0.1 T. In addition, a series of  $ac-\chi$  experiments were performed with various measuring frequencies. The static magnetization was obtained using a dc extraction method. Both types of measurements were carried out in a demagnetization cryostat.

The neutron diffraction experiments were performed at the DIB Multicounter Diffractometer of the Institut Laue-Langevin in Grenoble. Due to the extremely high absorption cross section  $\sigma$  of  $^{151}\text{Eu}$  we were forced to use samples enriched (99.2%) with  $^{153}\text{Eu}$ , and even this isotope has  $\sigma = 400$  b for thermal neutrons.

## III. EXPERIMENTAL RESULTS

### A. Ac susceptibility

The low-field, low-frequency differential magnetic mass susceptibility,  $\chi/\rho$  ( $\rho =$  density), is shown in Fig. 1 as a function of temperature  $T$  at low  $T$  for four samples of  $\text{Eu}_x\text{Sr}_{1-x}\text{S}$  with  $x = 0.10, 0.25, 0.30$ , and  $0.40$ . The predominant features of these curves are rather strong maxima whose intensity and position increase with concentration, whereas  $\chi$  at  $T \rightarrow 0$  K stays nearly constant. The temperature of the maximum is used to define a critical temperature called  $T_f$ , and these values are plotted in Fig. 2 together with the Curie temperatures  $T_C$ <sup>10</sup> as a function of the Eu concentration  $x$  in the whole series  $\text{Eu}_x\text{Sr}_{1-x}\text{S}$ . There is an almost linear increase of  $T_f$

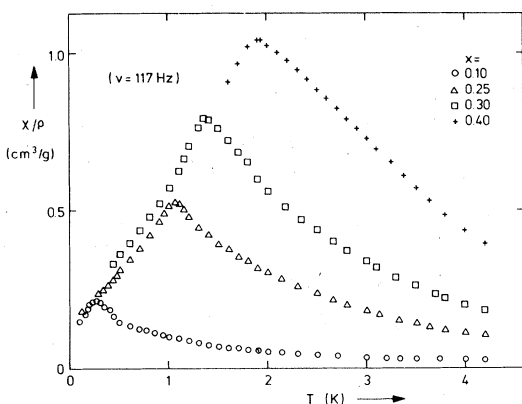


FIG. 1. Temperature dependence of the ac susceptibility in  $\text{Eu}_x\text{Sr}_{1-x}\text{S}$  with different Eu concentration  $x$ .

with  $x$  up to about  $x=0.50$ , changing to a much steeper and nonlinear increase of the ferromagnetic ordering temperature  $T_C$  at higher concentrations.

At this point it might be interesting to note that the high-temperature susceptibility of these samples measured with the help of a Faraday balance<sup>13</sup> follows a Curie-Weiss law  $\chi = C/(T - \theta)$ , with a Curie constant  $C$  in good agreement with the free-ion value

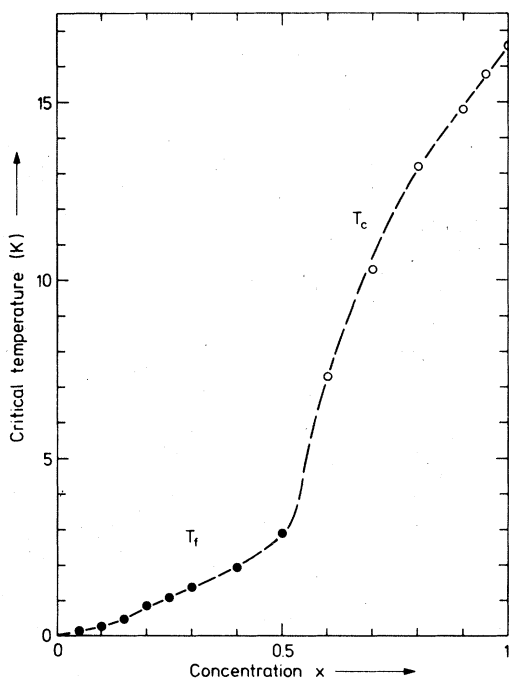


FIG. 2. Concentration dependence of the ordering temperatures (Curie temperature  $T_C$ , spin-glass temperature  $T_f$ ) in  $\text{Eu}_x\text{Sr}_{1-x}\text{S}$ .  $T_f$  is determined by ac susceptibility measurements using 117 Hz.

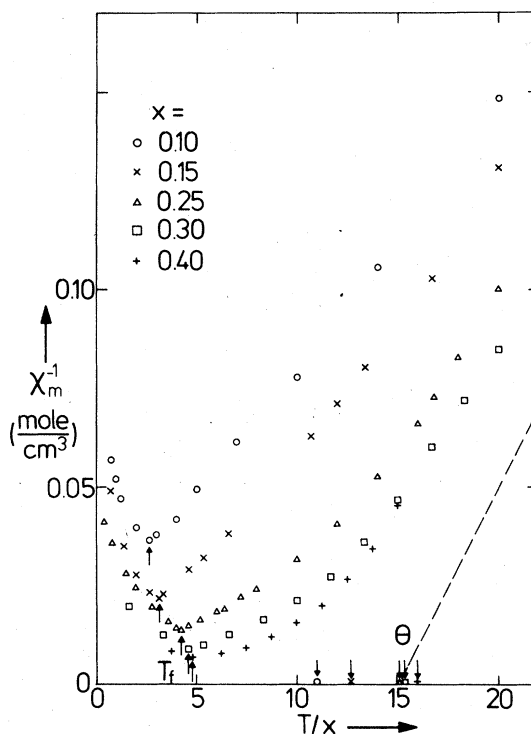


FIG. 3. The reciprocal molar susceptibility (ac- $\chi$ ),  $\chi_m^{-1}$ , in  $\text{Eu}_x\text{Sr}_{1-x}\text{S}$  as a function of the concentration-scaled temperature,  $T/x$ . The minima of the curves ( $T_f$ ) are indicated by upward arrows. For comparison, the slope of the high-temperature Curie-Weiss behavior  $\chi_m^{-1}(T)$  with the corresponding paramagnetic  $\theta$  (downward arrows) for various concentrations  $x$  is shown, too.

of  $\text{Eu}^{2+}$ , and a paramagnetic Curie-Weiss temperature  $\theta$  being positive over the whole concentration regime  $0 < x \leq 1$ . Therefore, under the reasonable assumption of no drastic change of  $J_1$  and  $J_2$  with  $x$ , the maximum in  $\chi(T)$  observed cannot be interpreted as a transition into an antiferromagnetically ordered state.

At lower temperatures, however, strong deviations from the Curie-Weiss behavior of  $\chi$  are measured, as shown in Fig. 3. The plot of the reciprocal molar susceptibility  $\chi_m^{-1}$  versus the concentration-scaled temperature  $T/x$  is motivated by the fact that at high temperatures  $\chi_m^{-1}(T/x)$  exhibits straight lines with the same slope, extrapolating to slightly different intersections with the abscissa. The values of  $\theta(x)$  and the Curie-Weiss slope are indicated in Fig. 3 for comparison, together with the low-temperature  $\chi$  behavior. The measurements demonstrate a systematic, concentration-dependent deviation from the high-temperature linear behavior, which presumably is connected with a ferromagnetic, short-range clus-

tering of the Eu moments well above the critical temperature  $T_f$ . The values of  $\chi(T_f)/x$  and  $\theta/T_f$  are found to be nearly independent of the concentration  $x$ .

### B. Neutron diffraction

In order to obtain direct information on the type of magnetic order below  $T_f$  in  $\text{Eu}_x\text{Sr}_{1-x}\text{S}$  for  $x \leq 0.5$  we have performed neutron-diffraction measurements on  $^{153}\text{Eu}$  enriched samples. Any periodical spin structure must be reflected in the magnetic diffraction pattern characterized by sharp peaks of the scattered intensity at the Bragg angles of the magnetic lattice. In such an experiment, however, one also has to take into account the elastic neutron scattering on the nuclei resulting in sharp Bragg peaks from the crystal structure, and the diffuse elastic scattering from the different nuclei, as well as from the distribution of the magnetic atoms in such substituted compounds. For the investigation of the type of magnetic order one can get rid of all the other nonrelevant contributions to the elastic scattering by taking the difference of the intensity measured below and above the ordering temperature.

As an example, Fig. 4 shows two measurements on  $\text{Eu}_{0.4}\text{Sr}_{0.6}\text{S}$  at temperatures of 1.3 and 60 K, corrected for the background and the vanadium can. For this sample the ac susceptibility yields  $T_f = 1.92$  K. The high-temperature pattern solely displays sharp peaks at the first three Bragg angles (111), (200), and (220) of the NaCl crystal structure,

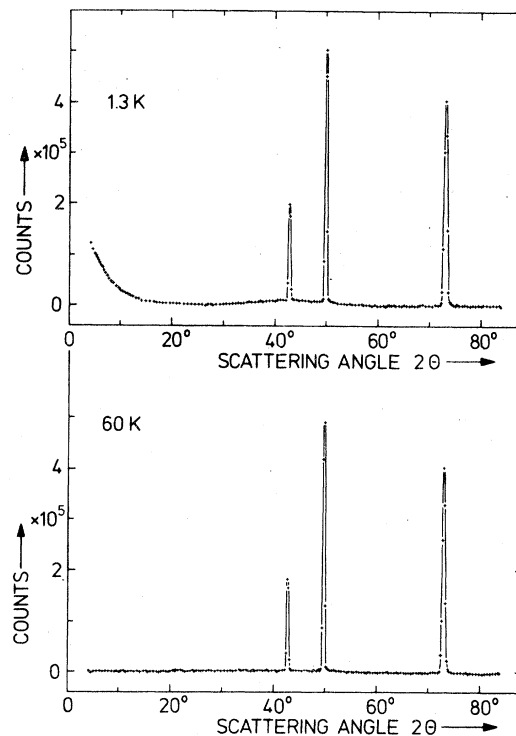


FIG. 4. Neutron-diffraction spectra of  $\text{Eu}_{0.40}\text{Sr}_{0.60}\text{S}$  at temperatures of 1.3 and 60 K, after correction for background.

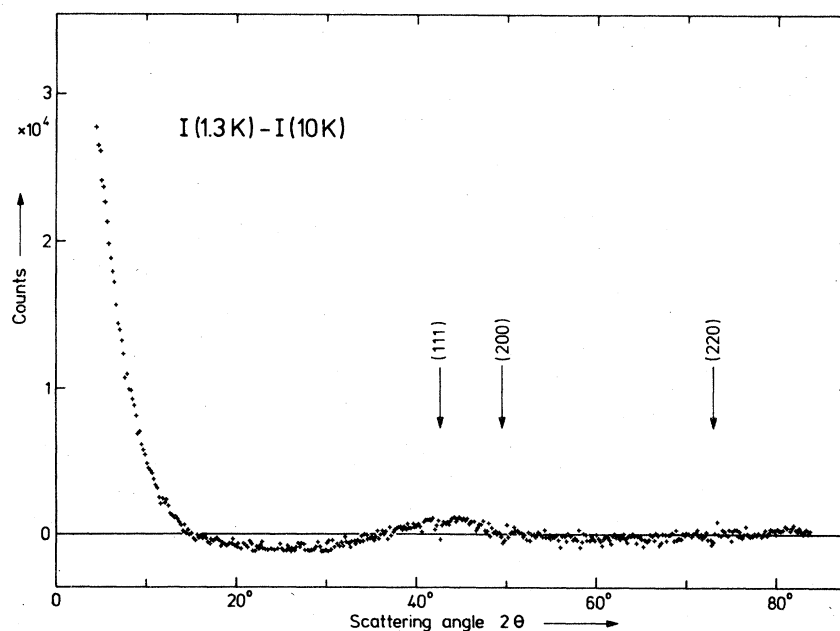


FIG. 5. Difference between two neutron-diffraction spectra at 1.3 K ( $T < T_f$ ) and 10 K ( $T > T_f$ ) as a function of the scattering angle  $2\theta$  in  $\text{Eu}_{0.4}\text{Sr}_{0.6}\text{S}$ . The positions of the first three Bragg angles in the NaCl lattice are indicated.

whereas at 1.3 K additional intensity appears originating from diffuse scattering at small angles and around the first Bragg angles. Figure 5 shows that in the difference between two such spectra recorded below and above the critical temperature  $T_f$  no sharp lines are left either at the Bragg angles (indicated by arrows in Fig. 5) nor elsewhere within the range of angles covered. This demonstrates that there is no onset of long-range order at  $T_f$  in the sample. Instead one can identify in the figure a steep increase of the diffuse scattering intensity at low angles, together with a broad bump around the first Bragg angles, indicating short-range ferromagnetic ordering. This magnetic diffuse scattering sets in at a much higher temperature than  $T_f$  and is temperature and concentration dependent, in consistency with the short-range coupling above  $T_f$  observed in the  $\chi$  measurements (see Sec. III A).

### C. Static magnetization

The magnetic properties below  $T_f$  of the  $\text{Eu}_x\text{Sr}_{1-x}\text{S}$  samples were further explored by static magnetization measurements in low fields and at very low temperatures. Magnetization curves for  $x = 0.40$  are shown in Fig. 6. A short note on this investigation has al-

ready been presented at a conference.<sup>14</sup> First of all no spontaneous magnetization could be detected below  $T_f$  after zero-field cooling. At low temperatures such virgin magnetization curves (zero-field cooling, increasing field) differ from those of paramagnets in three features: (i) the initial susceptibility increases with increasing temperature, (ii) the curves are distinctly S shaped, and (iii) they cross in higher fields.

The first observation leads to the maximum in the low-field susceptibility in dependence on temperature as also has been measured with the help of the ac technique. The second feature results in an inflection point of the curve at an external field  $B^m$  which is temperature and concentration dependent. With increasing temperature the inflection point moves steadily downward in field and disappears at about the critical temperature  $T_f$ . The values of  $B^m$  increase with the Eu concentration. No tendency towards saturation of the magnetization is observable, even at the lowest temperature, within the range of the applied fields up to 0.4 T.

Another type of magnetization measurements was carried out after field cooling, i.e., each point  $\sigma(B_0, T)$  was measured after applying a finite field  $B_0$  at a temperature  $T^* > T_f$  and subsequently cooling the sample in this field  $B_0$  down to the temperature

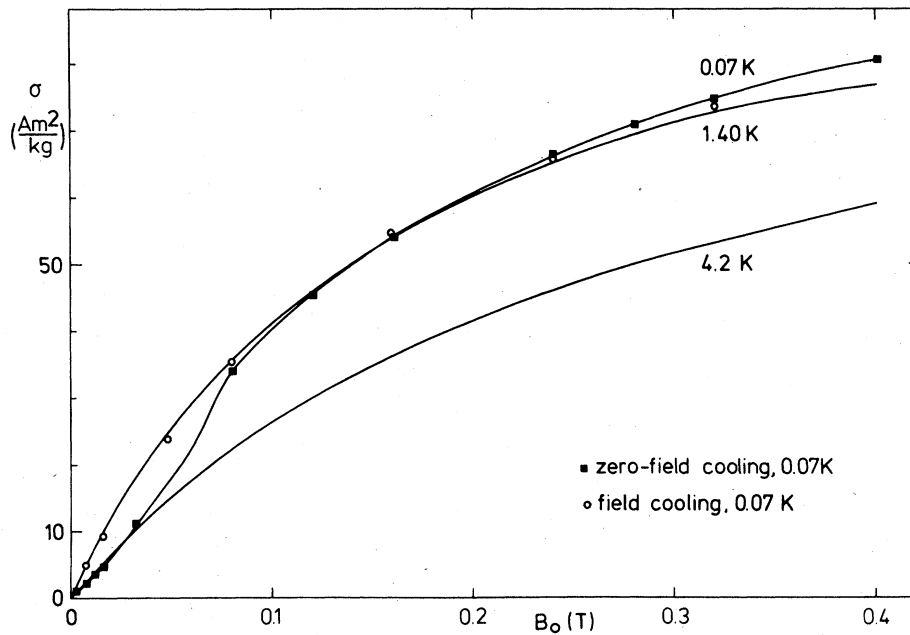


FIG. 6. Field ( $B_0$ ) dependence of the magnetization ( $\sigma$ ) in  $\text{Eu}_{0.4}\text{Sr}_{0.6}\text{S}$  measured at three temperatures  $T = 4.2, 1.4,$  and  $0.07$  K in increasing field after cooling in zero field (solid lines; the curve at  $T = 0.07$  K is marked with black squares). In addition a fourth series of measurement is displayed by open circles where each point of  $\sigma(B_0)$  has been obtained at  $0.07$  K after cooling in a certain field  $B_0$  from above  $T_f$  down to  $0.07$ .

$T < T_f$ . One of these series is shown in Fig. 6 (open circles) measured on a sample with  $x = 0.40$  at  $T = 70$  mK. As one can identify the peculiarities, discussed above for the virgin curves, disappear due to the cooling procedure in finite fields.

In this connection, it is very interesting to report on the remanent magnetization measured on these samples. Again, two different procedures were applied. First, the sample was cooled down to  $T < T_f$  in zero field, then the field was raised to a value  $B_0$  and the remanent magnetization was measured immediately after switching off the field  $B_0$  at  $T$ . This procedure was repeated for different values of  $B_0$  resulting in the isothermal remanent magnetization (IRM) displayed in Fig. 7 for  $T = 70$  mK and  $x = 0.30$ . The second way to find a remanence is to measure each point after field cooling, determining the thermoremanent magnetization (TRM). The TRM clearly develops much stronger than the IRM with field (Fig. 7) and goes through a maximum, but ultimately both curves saturate at the same value.

The values of the remanent magnetization exhibit a simple concentration dependence. The maximum measured in the TRM,  $\sigma_{TRM}^m$ , as shown in Fig. 7 at 70 mK, is related to the saturation magnetization  $\sigma_0$  calculated for the free-ion value of  $\text{Eu}^{2+}$  by

$$\sigma_{TRM}^m = 0.15 \cdot \sigma_0 \cdot x \tag{1}$$

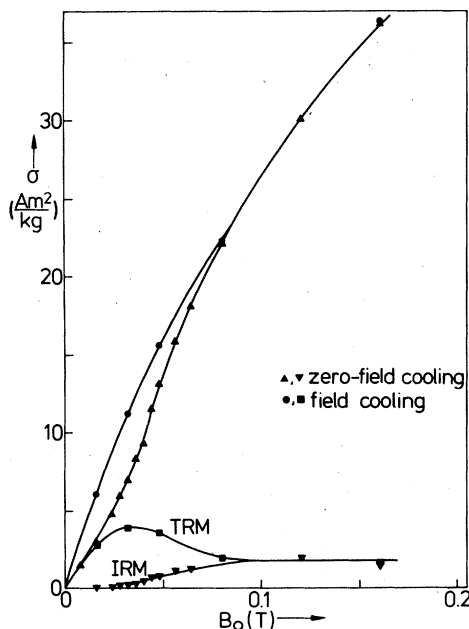


FIG. 7. Low-field magnetization of  $\text{Eu}_{0.3}\text{Sr}_{0.7}\text{S}$  at 0.07 K. Both the magnetization  $\sigma$  and isothermal remanent magnetization (IRM), measured after zero-field cooling in increasing field, as well as the magnetization  $\sigma_B$  and the thermoremanent magnetization (TRM), measured after cooling in the field  $B_0$ , are shown.

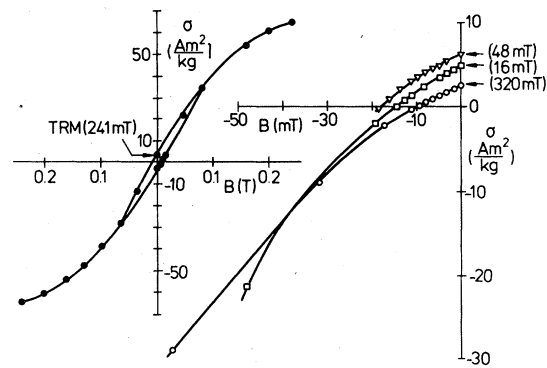


FIG. 8. On the right: Dependence of several thermoremanent magnetizations (TRM) on low inverse fields (opposite to the fields applied during the cooling process with magnitudes as indicated on the vertical axis) in  $\text{Eu}_{0.4}\text{Sr}_{0.6}\text{S}$  at 0.07 K. On the left: Magnetic hysteresis loop of  $\text{Eu}_{0.4}\text{Sr}_{0.6}\text{S}$  at 0.07 K, starting with the thermoremanent magnetization (TRM) after cooling in a field of 0.241 T.

and the saturation value of both remanent magnetizations (RM),  $\sigma_{RM}^{sat}$  is found to be

$$\sigma_{RM}^{sat} = 0.47 \cdot \sigma_{TRM}^m \tag{2}$$

The values of the magnetic fields, corresponding to the maximum in the TRM, also increase with the Eu concentration and are found to coincide with the position of the inflection points  $B^m$  of the virgin magnetization curves.

After measuring the TRM at 0.07 K its reduction by an inverse magnetic field was investigated (the

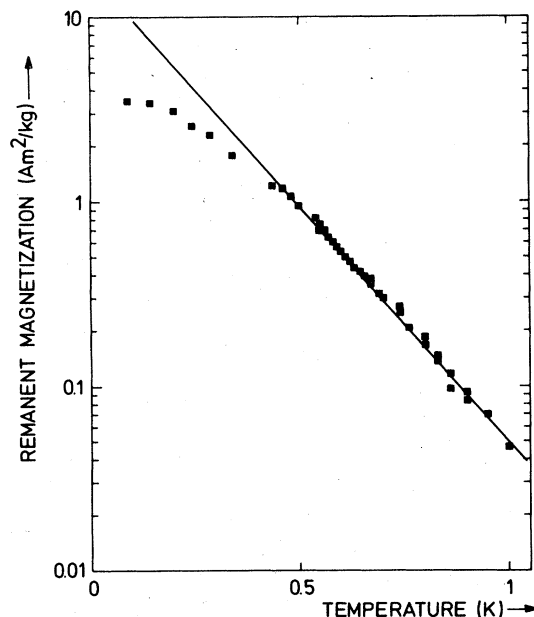


FIG. 9. Temperature dependence of the saturated remanent magnetization in  $\text{Eu}_{0.4}\text{Sr}_{0.6}\text{S}$ .

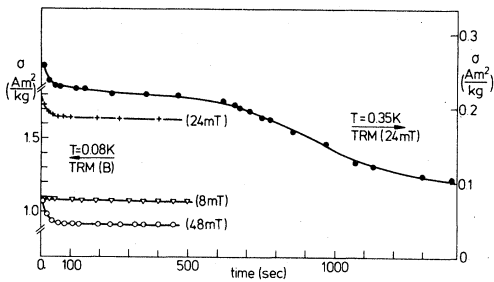


FIG. 10. Time dependence of the thermoremanent magnetization (TRM) in  $\text{Eu}_{0.2}\text{Sr}_{0.8}\text{S}$ . Full circles:  $T = 0.35$  K, cooling field 24 mT. Other symbols: initial decay at  $T = 80$  mK, cooling fields as indicated within the brackets.

plus direction of  $B_0$  is that of the field applied during cooling). From the result of the sample with  $x = 0.40$  (Fig. 8) one realizes the coercive fields to be small. For one of the TRM, measured after switching off the field of 241 mT (millitesla), a full hysteresis loop was investigated. It was found to be narrow and symmetrical around zero (Fig. 8).

The samples further reveal their nature by displaying significant temperature- and time-dependent effects of the remanent magnetization. Figure 9 shows the saturated remanent magnetization in  $\text{Eu}_{0.4}\text{Sr}_{0.6}\text{S}$ , measured immediately after switching off the magnetic field, as a function of temperature. The data follow a simple exponential law above 0.4 K, but not below. In Fig. 10 we have plotted the time dependence of the TRM in  $\text{Eu}_{0.2}\text{Sr}_{0.8}\text{S}$ . After an initial rapid decay we obtain a slowly decreasing TRM, changing also with temperature. The stronger initial decay

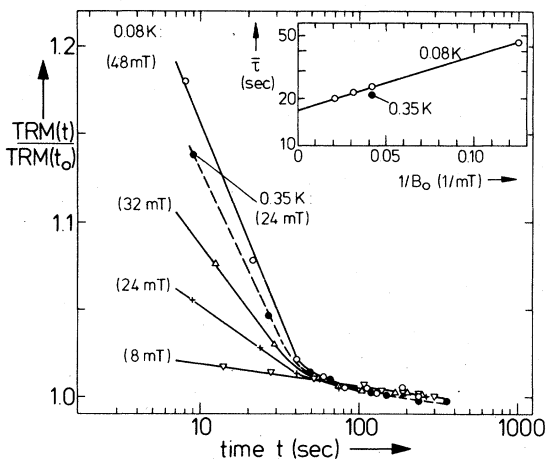


FIG. 11. Initial time decay of several thermoremanent magnetizations (TRM) (normalized to the value at  $t_0 = 200$  sec) in  $\text{Eu}_{0.2}\text{Sr}_{0.8}\text{S}$ , measured at 0.08 and 0.35 K after cooling in different fields (indicated within the brackets). The insert shows the mean relaxation times, estimated from these curves, in dependence on the reciprocal cooling field  $1/B_0$  (see discussion).

of the TRM with time, displayed in detail in Fig. 11, is found to be influenced by the previously applied cooling field.

#### D. Field effects on $T_f$

In order to study the nature of the transition at  $T_f$  in  $(\text{Eu},\text{Sr})\text{S}$ , detailed measurements of the magnetic susceptibility  $\chi$  in the vicinity of  $T_f$  were carried out. First, the magnetic field dependence of ac- $\chi$  was measured by superposing a static magnetic field up to 0.1 T. This revealed that the maxima of the susceptibility are very sensitive even to small external fields. Figure 12 shows the relative decrease of  $\chi_{\text{max}}$  with the applied static fields  $B_0$  in  $\text{Eu}_x\text{Sr}_{1-x}\text{S}$  samples with Eu concentrations  $x = 0.15, 0.25, 0.30,$  and  $0.40$ . The data exhibit a nearly concentration-independent behavior, especially at low fields.

We also observe a second effect: the maximum of ac- $\chi$  not only becomes weaker and broader, but it also moves to lower temperatures relative to the zero-field maximum at  $T_f(0)$  as the external field  $B_0$  is increased. The relative shift of the peak position  $T_f$  is stronger in the samples with higher-Eu concentration  $x$ , as shown in Fig. 13. The measured initial shift can be expressed by

$$1 - T_f(B_0)/T_f(0) = (0.04 \text{ mT}^{-1}) \cdot x \cdot B_0 \quad (3)$$

for  $x \cdot B_0 \leq 5 \text{ mT}$ ,

where the values of  $B_0$  have to be taken in mT. As an example, a downward shift of 20% in the peak position is already obtained by applied fields of 33, 20, and 17 mT in  $\text{Eu}_x\text{Sr}_{1-x}\text{S}$  with  $x = 0.15, 0.25,$  and  $0.30$ , respectively. A different behavior is observed in  $\text{Eu}_{0.4}\text{Sr}_{0.6}\text{S}$ . There the position of  $\chi_{\text{max}}$  is initially shifted upwards, and with somewhat higher fields it

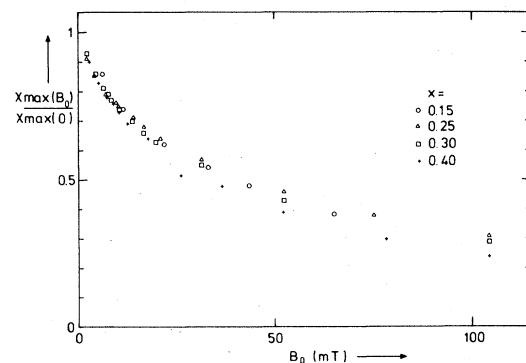


FIG. 12. Field dependence of the susceptibility maximum,  $\chi_{\text{max}}(B_0)$ , normalized to  $\chi_{\text{max}}(B_0 = 0)$ , as measured by the ac-method (117 Hz,  $10^{-5}$  T) with superposed small static magnetic fields  $B_0$  in  $\text{Eu}_x\text{Sr}_{1-x}\text{S}$  with  $x = 0.15, 0.25, 0.30,$  and  $0.40$ .

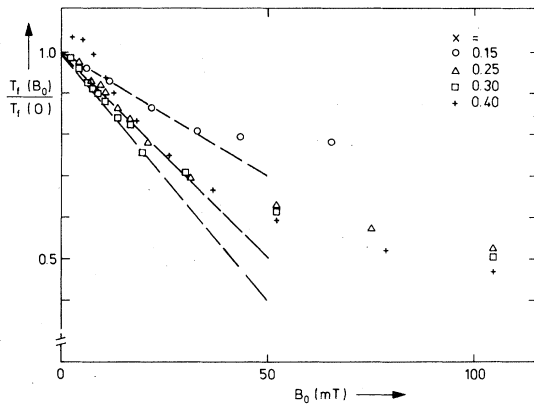


FIG. 13. Field dependence of the position of the susceptibility maximum,  $T_f(B_0)$ , in  $\text{Eu}_x\text{Sr}_{1-x}\text{S}$  (the experimental details are the same as described in the caption of Fig. 12).

again changes to a downward shift, as displayed in Fig. 13. It is possible that this different behavior of  $x = 0.40$  is due to the vicinity of the spin-glass-to-ferromagnetism transition ( $x_c \approx 0.5$ ) which is currently under investigation.

#### E. Time effects on $T_f$

In  $(\text{Eu},\text{Sr})\text{S}$  the maximum of  $\chi$  derived from the static magnetization in low fields ( $10^{-3}$  T) is found to be systematically at a lower temperature than  $T_f$  determined by the ac- $\chi$  measurement on the same sample. The results of both kinds of measurements are displayed in Fig. 14. To pursue this, a series of ac- $\chi$  experiments has been performed with various measuring frequencies. Consistent with the observation shown in Fig. 14 the position of  $\chi_{\text{max}}$  is shifted

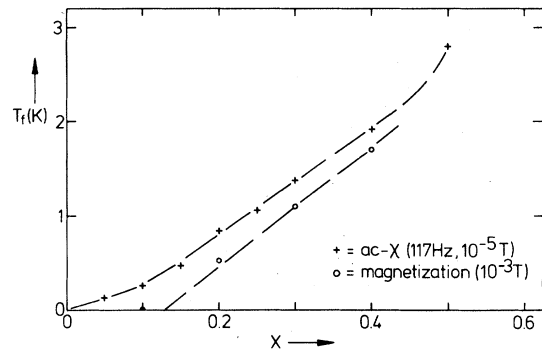


FIG. 14. Concentration dependence of the spin-glass temperature  $T_f$  in  $\text{Eu}_x\text{Sr}_{1-x}\text{S}$  for  $x \leq 0.5$ , as determined by the maximum of the susceptibility either in a low-frequency, low-field differential  $\chi$  measurement (117 Hz,  $10^{-5}$  T) or in a low-field, static magnetization measurement ( $10^{-3}$  T).

downwards by lowering the frequency of the ac- $\chi$  measurement. Some of the results are compiled in Table I. In Fig. 15 we have plotted  $(T_f^{\text{ac}})^{-1}$  as a function of  $\log \nu$  for various concentrations  $x$ . Within the frequency range available, our results can be represented by the relation

$$(T_f^{\text{ac}})^{-1} = -S(x) \cdot \log \nu, \quad (4)$$

where the slope  $S(x)$  increases with decreasing concentration  $x$ . In an attempt to compare the dc and ac susceptibility measurements, the  $T_f$  values obtained from the ac method have been extrapolated to  $\nu = 0.02$  Hz, the measuring frequency estimated for the static (dc) method (see Fig. 15). These values,  $T_f^{\text{ac}\phi}$ , are still higher than the freezing temperatures measured in the static magnetization, as shown in Fig. 15 and Table I.

TABLE I. Temperatures (K) of the susceptibility maximum in  $(\text{Eu}_x\text{Sr}_{1-x})\text{S}$  measured by a dc method ( $10^{-3}$  T) and an ac method ( $10^{-5}$  T) using various measuring frequencies.

$x =$	dc	ac $\phi$ (0.02 Hz) <sup>a</sup>	ac (12 Hz)	ac (117 Hz)	ac (4200 Hz)	$E_a$ (K) <sup>b</sup>
0.10	<0.08	0.22	0.260	0.267	0.295	9
0.15			0.433	0.463	0.530	19
0.20	0.52	0.70	0.807	0.840	0.920	36
0.25			1.040	1.065	1.130	68
0.30	1.10	1.25	1.350	1.380	1.450	111
0.40	1.70	1.79	1.880	1.920	2.000	204

<sup>a</sup>Extrapolated values as described in the text.

<sup>b</sup>Anisotropy energy derived from an Arrhenius plot.

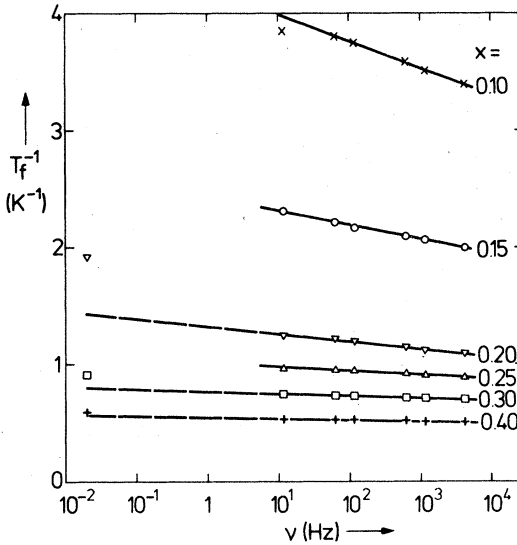


FIG. 15. Inverse temperature of the ac susceptibility maximum,  $(T_f^{ac})^{-1}$ , as function of the measuring frequency  $\nu$  for various Eu concentrations  $x$  in  $\text{Eu}_x\text{Sr}_{1-x}\text{S}$ . In addition the  $T_f^{dc}$  values measured by the dc susceptibility are shown at  $\nu = 0.02$  Hz.

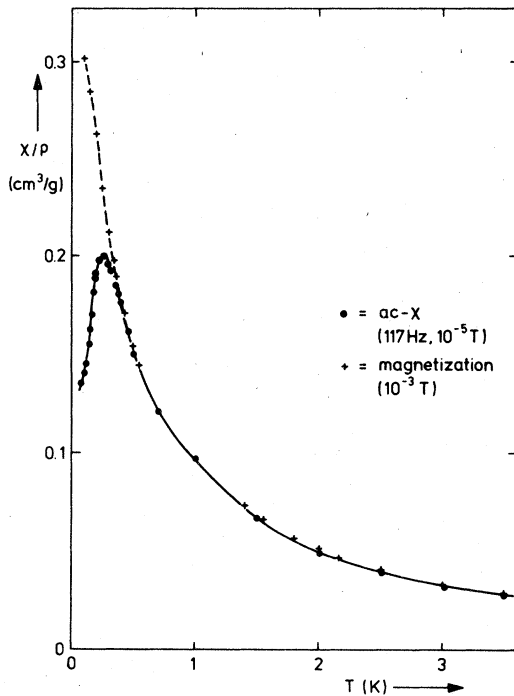


FIG. 16. Temperature dependence of the magnetic susceptibility in  $\text{Eu}_{0.1}\text{Sr}_{0.9}\text{S}$  as measured by an ac-X method (117 Hz,  $10^{-5}$  T) and by a low-field ( $10^{-3}$  T), static magnetization experiment.

#### F. Transition at low concentration

A special situation has been observed for the sample  $\text{Eu}_{0.1}\text{Sr}_{0.9}\text{S}$ . The maximum of the ac susceptibility (measured with a frequency of 117 Hz and an amplitude of  $10^{-5}$  T) appears at  $T = 0.26$  K, whereas in the static magnetization with an external field of  $10^{-3}$  T no maximum could be detected down to the lowest temperature of 0.08 K (see Fig. 16). This astonishing finding is now under further investigation, e.g., in lower external fields and down to lower temperatures. The results will be published in detail soon, together with a theoretical investigation of  $\chi(T)$  in this low-concentration regime.<sup>15</sup>

### IV. DISCUSSION

#### A. (Eu,Sr)S, an insulating spin-glass system

The experimental results on  $\text{Eu}_x\text{Sr}_{1-x}\text{S}$  for  $x \leq 0.5$  described above reveal some basic characteristics of spin glasses: The initial ac susceptibility shows a maximum at a temperature  $T_f$ , called freezing temperature, below which there is no long-range magnetic order, as proved by neutron diffraction. This technique, together with the deviations from the Curie-Weiss behavior measured in  $\chi(T)$ , exhibits the onset of short-range ferromagnetic ordering above  $T_f$ . Below  $T_f$  remanent magnetizations are observed, depending on the thermomagnetic history, with a characteristic slow, nonexponential time decay. The susceptibility at  $T \rightarrow 0$  K is found to be finite.

Our systematic experimental work on these nonmetallic samples supports the idea that the RKKY interaction via the conduction electrons may not be considered as a necessary condition for spin-glass properties. In the insulator EuS two kinds of exchange interactions with opposite sign are responsible for the overall ferromagnetic ordering below 16.6 K as described in the Introduction. These interactions are basically shorter in range than the coupling via conduction electrons. Presumably random competing ferro- and antiferromagnetic interactions as present in (Eu,Sr)S are the essential condition for spin-glass properties. The fundamental consequence that not all interactions can be satisfied simultaneously has been recently<sup>16</sup> called "frustration" and may help to unify theoretical treatments of the spin-glass properties.<sup>17,18</sup>

Comparing the (Eu,Sr)S samples with the canonical spin-glass system  $\text{AuFe}$ , the most striking properties of our system are the relatively low-transition temperatures  $T_f$  and the high concentrations  $x$  of magnetic atoms. As a measure, we consider the ratio  $T_f/x$ , with

$$T_f/x \approx 5 \text{ K}, \quad (5)$$

in  $\text{Eu}_x\text{Sr}_{1-x}\text{S}$  as compared to  $T_f/x \approx 1000$  K in  $\text{AuFe}$ .<sup>19</sup> Taking into account the frustration effects, however, it is more convenient to compare the product  $P(0) \cdot T_f/x$  for different spin glasses, where  $P(0)$  is the density of vanishing effective coupling and therefore a measure of the correlations between spin directions and signs of the interactions. Following Ref. 18 one has the relation

$$P(0) \cdot T_f/x = \chi(0) \cdot T_f/(\mu^2 \cdot x) \quad (6)$$

and this expression is equal in magnitude to both systems at low concentrations [e.g., for 0.2 at. % Fe in Au (Ref. 19) and 15% EuS in SrS].

One should note the high concentration of magnetic atoms within the spin-glass regime in  $\text{Eu}_x\text{Sr}_{1-x}\text{S}$  with a critical concentration  $x_c$  for the onset of long-range ferromagnetism<sup>20</sup> of

$$x_c \approx 0.5, \quad (7)$$

compared to  $x_c \approx 0.16$  in  $\text{AuFe}$ . This will be further discussed below.

Increasing the Eu concentrations  $x$  within the spin-glass regime enhances the tendency towards ferromagnetism, reflected in the steady growth of the positive Curie-Weiss temperature and of the susceptibility at  $T_f$ . Nevertheless, the saturation values of the remanent magnetization observed remain only a few percent of the saturation magnetization (like in metallic spin glasses), even for the high-Eu concentrations, and are simply related to the concentration [see Eqs. (1) and (2)]. This suggests that the moments on the Eu atoms are nearly randomly oriented. We recall that the freezing temperature  $T_f$  increases nearly linearly with concentration. Probably these simple concentration dependences are caused by the predominant short-ranged nature of the exchange interactions underlying in the (Eu,Sr)S spin-glass system.

### B. Magnetic properties below $T_f$

First of all the results of the low-field, low-temperature magnetization measurements below  $T_f$  will be discussed with emphasis on the reversible and irreversible properties of the spin-glass state. Figure 7 gives an example of our result that the virgin magnetization  $\sigma(B, T)$  for small magnetic fields  $B$  at temperatures  $T \leq T_f$  fulfills the following equation:

$$\sigma(B, T) = \sigma_B(T) - \text{TRM}(B, T) + \text{IRM}(B, T), \quad (8)$$

where  $\sigma_B(T)$  is the magnetization measured at  $T$  after cooling the sample in the field  $B$  from above  $T_f$  down to  $T$ . The S-shaped curvature of the virgin magnetization, therefore, is directly connected to the field dependence of the remanences. This is further demonstrated by the observation that the field at the

inflection point  $B^m$  coincides with that at the maximum of the TRM.

Comparing the field-cooled magnetization with the virgin curves one realizes not only the disappearance of the inflection point after field cooling (Fig. 6) but the coincidence of the curve with the magnetization measured at  $T = T_f$ , i.e.,

$$\sigma_B(T) = \sigma(B, T) \quad \text{for } T \leq T_f. \quad (9)$$

The temperature dependence of both types of magnetizations,  $\sigma(B, T)$  and  $\sigma_B(T)$ , in small external fields corresponds to the thermal variation of the reversible and irreversible susceptibilities,  $\chi_{\text{rev}}$  and  $\chi_{\text{irr}}$ , respectively:  $\chi_{\text{rev}}$  increases with temperature up to  $T_f$ , but the sum of  $\chi_{\text{rev}}$  and  $\chi_{\text{irr}}$  stays constant below  $T_f$ ,

$$\chi_{\text{rev}}(T) + \chi_{\text{irr}}(T) = \chi(T_f) \quad \text{for } T \leq T_f, \quad (10)$$

where

$$\chi_{\text{rev}} = \lim_{B \rightarrow 0} d\sigma(B, T)/dB, \quad (11)$$

$$\chi_{\text{irr}} = \lim_{B \rightarrow 0} d\sigma(\text{TRM})/dB. \quad (12)$$

These properties have already been observed in metallic spin glasses like  $\text{AuFe}$  by Tholence and Tournier in 1974.<sup>5</sup> A recent Monte Carlo simulation of a two-dimensional Ising spin glass<sup>21</sup> seems to reproduce the behavior described above. The maximum in the TRM over  $B$ , observed in (Eu,Sr)S as well as in metallic spin glasses, is found in the computer simulation, too.

Saturation of the remanences (when the TRM is equal to the IRM) is reached even in small magnetic fields in (Eu,Sr)S in contrast to the behavior in metallic spin glasses, but always at fields three to four times larger than  $B^m$ , the field for the maximum in the TRM. As an example, Fig. 7 exhibits

$$B^m = 0.03 \text{ T in } \text{Eu}_{0.3}\text{Sr}_{0.7}\text{S}, \quad (13)$$

whereas in  $\text{Fe}_{0.005}\text{Au}_{0.995}$  Ref. 5 shows  $B^m = 0.35$  T. The experiments on  $\text{Eu}_x\text{Sr}_{1-x}\text{S}$  yield values of  $B^m$  increasing with the Eu concentration  $x$ , as the spin-glass temperature  $T_f$  does, too. For the ratio between the applied field  $B^m$  and the interaction energy  $k_B T_f$ , we find a unique value of

$$\mu B^m / (k_B T_f) = 0.14 \quad (14)$$

independent of concentration for (Eu,Sr)S as well as for the published data on metallic spin glasses, assuming contributions of individual magnetic moments  $\mu$ . Then the minimum field  $B^{\text{sat}}$  necessary to saturate the remanence states fulfills the relation

$$\mu B^{\text{sat}} = 0.5 \cdot k_B T_f, \quad (15)$$

apparently independent of concentration and of the type of interaction. One has to point out that no in-

dication of the formation of giant moments is detected in these remanence measurements.

An interesting experimental result in the (Eu,Sr)S samples is the dependence of the thermoremanent magnetization on the previously applied magnetic field (during the cooling process), which exhibits a much more pronounced maximum than in canonical spin-glass samples [see Fig. 7 and Eq. (2)]. As a quite peculiar result, the same TRM values can be observed by cooling the sample in a small ( $B < B^m$ ) or a high ( $B > B^m$ ) external field, relative to the field  $B^m$  at the maximum of the TRM. Several properties, however, demonstrate the difference between such two metastable states. First of all, in an inverse magnetic field the saturated remanent magnetization appears to be relatively harder as shown in Fig. 8 ( $B^m \approx 40$  mT in  $\text{Eu}_{0.4}\text{Sr}_{0.6}\text{S}$  at 70 mK). Moreover, we observe a markedly different time dependence: for instance, in Fig. 10 both TRM values for the cooling fields of 8 and 48 mT in  $\text{Eu}_{0.2}\text{Sr}_{0.8}\text{S}$  at 80 mK ( $B^m \approx 20$  mT) are only equal immediately after switching off the field ( $\sim 8$  sec), but the TRM (48 mT) decays to a lower magnetization more quickly.

The anomalously slow relaxation observed in the magnetization and the remanence of (Eu,Sr)S on a time scale of several minutes or hours is known as a characteristic feature of spin glasses. Figure 10 displays the typical nonexponential time decay of the TRM in  $\text{Eu}_{0.2}\text{Sr}_{0.8}\text{S}$  at  $T = 0.35$  K, where half of the value of TRM at  $t = 0$  is reached only after 18 min. Similar time dependences have already been measured in a very dilute (Eu,Sr)S sample by Holtzberg *et al.*<sup>22</sup> After several minutes the remanence reaches a metastable state which obviously decays very slowly with time, especially at very low temperatures [see TRM (24 mT) in Fig. 10]. In order to characterize the stronger initial decay with time, a mean relaxation time  $\bar{\tau}$ , defined as that time required for the decay to half the value of the difference [TRM( $t = 0$ ) - TRM( $t = 200$  sec)], is estimated from Fig. 11. The resulting relaxation times are shown in the insert of Fig. 11. Clearly, the initial time decay of the TRM is stronger after cooling in higher fields and at increased temperature. Note that no anomaly is detected around the maximum value of the TRM ( $B^m \approx 20$  mT).

The experimental data discussed above may help to understand the maximum in the thermoremanent magnetization TRM measured in dependence of the cooling field in spin-glass samples. It seems reasonable to trace back this effect to the different time decays. Hence we would suggest that the maximum is less pronounced if the TRM is measured more quickly after switching off the cooling field. A detailed theoretical study on that phenomenon by Kinzel,<sup>21</sup> using Monte Carlo simulations of the Edwards-Anderson model, will be published soon.

In the phenomenological model for spin glasses cit-

ed above, where the blocking of superparamagnetic clouds is treated according to Néel's work on rock magnetism,<sup>5</sup> the thermal variation of the saturated remanent magnetization is derived to show an exponential decrease. In canonical spin glasses like *AuFe* and *CuMn*, such a temperature dependence has in fact been measured,<sup>22</sup> whereas our results on (Eu,Sr)S (Fig. 9) reveal a deviation from the exponential law at low temperatures. We suggest that this nonexponential behavior is again an effect depending on the measuring time and therefore may be directly connected with the pronounced maximum in the TRM.

Mainly because of those irreversible magnetic properties which are common to spin glasses, several authors<sup>5,23</sup> have put forward the phenomenological model which describes spin-glass behavior in terms of the blocking of superparamagnetic clusters, leading to nonequilibrium metastable states at low temperatures. The question arises whether there is a phase transition in spin glasses at all. We think a detailed experimental investigation of the susceptibility around  $T_f$  in (Eu,Sr)S may contribute to the study of this problem, as will be discussed in Sec. IV C-E.

### C. Field effects on $T_f$

The measurements of the magnetic susceptibility  $\chi$  near  $T_f$  in (Eu,Sr)S demonstrate the extreme sensitivity of  $\chi(T_f)$  and of  $T_f$  to small external magnetic fields. Even small fields cause the maximum of the ac susceptibility to become weaker, as shown in Fig. 12. Similar features have already been observed in *AuFe* alloys by Cannella and Mydosh<sup>4</sup> and have been considered since that time as one of the characteristics of spin glasses. These authors reported a 10% reduction of  $\chi_{\text{max}}$  with  $B_0 = 20$  mT for Fe concentration between 1 and 8 at.%, and a stronger reduction for 13 at. % Fe in Au. The present work on (Eu,Sr)S reveals a stronger sensitivity of  $\chi_{\text{max}}$  to the applied field  $B_0$  (with  $B_0 = 20$  mT, we get a nearly 40% reduction of  $\chi_{\text{max}}$ ), and the behavior of the various samples seems to exhibit a universal curve independent of concentration  $x$  within the experimental error (Fig. 12). Taking into account, however, that the freezing temperature  $T_f$  increases with the Eu concentration  $x$ , the decrease of  $\chi_{\text{max}}$  is much stronger for higher Eu concentrations regarding the dependence on  $\mu B_0 / k_B T_f$ .

It should be noted that the ac susceptibility becomes nearly flat in a magnetic field required to saturate the remanent magnetization ( $\sim 0.1 T$ ). This demonstrates the correlation between the ac- $\chi$  maximum and the irreversible properties.

In *AuFe* no appreciable shift of the peak position was observed<sup>4</sup> in samples with 1 and 2 at. % Fe, whereas in samples with 5 and 8 at. % Fe  $\chi_{\text{max}}$  was

shifted upwards by about 1 K ( $\cong 4\%$ ) in fields of about 20 mT. On the other hand, our measurements on (Eu,Sr)S yield a downward shift of the susceptibility maximum with applied field (Fig. 13), which is more pronounced in samples with higher Eu concentrations. Very similar properties (decrease and downward shift of  $\chi_{\max}$ ) have recently been observed in the new spin-glass system  $(\text{La}_{1-x}\text{Gd}_x)\text{Al}_2$  with  $x = 0.04$ .<sup>24</sup> A downward shift of  $T_f$  with increasing magnetic field does not seem to be unreasonable, if one remembers that in a true antiferromagnet the disordering influence of an applied field also shifts  $T_N$  to lower values.

By increasing the Eu concentration  $x$  in  $\text{Eu}_x\text{Sr}_{1-x}\text{S}$ , as we have seen, the values of  $\chi(T_f)$  and of the paramagnetic Curie-Weiss temperature  $\theta$  increase nearly linearly, the regions of magnetically coupled spins grow in size, and hence the field effects on  $\chi(T_f)$  become stronger with  $x$  regarding the field strength relative to the interaction energy,  $\mu B_0/k_B T_f$ .

In an attempt to elucidate the nature of spin-glass ordering, Stauffer and Binder<sup>6</sup> have recently calculated the field dependence of the Edwards-Anderson order parameter  $q$  at  $T_f$  for an Ising model with a random (symmetric) nearest-neighbor exchange. Ac-

cording to the relation already obtained by Chalupa<sup>25</sup>

$$q \propto B^{2/\delta} \text{ at } T = T_f, \quad (16)$$

they determined the exponent  $\delta = 4.0$  in three dimensions by means of Monte Carlo simulations. Since  $q$  is related to the depression of  $\chi_{\max}$  with the applied field  $B$  by the relation

$$q(T_f) \propto 1 - \chi_{\max}(B)/\chi_{\max}(0), \quad (17)$$

we compare in Fig. 17 the theoretical result<sup>6</sup> with our experimental data on (Eu,Sr)S from Fig. 12, and find the same critical exponent  $\delta = 4.1$  for various Eu concentrations  $x$ . At present the reason for such a good agreement between our experimental result and the computer calculation is not clear to us. We feel that similar systematic work on metallic spin glasses is needed in order to draw any conclusion from this analysis.

#### D. Time effects on $T_f$

An interesting study concerning the time effects on the spin-glass transition  $T_f$  has already been published by Murani and Tholence<sup>26</sup>: in a Cu(8 at. % Mn) alloy they observed the maximum of  $\chi$  at  $39 \pm 1$  K in an ac- $\chi$  measurement, whereas a neutron scattering experiment revealed the spin-glass transition at  $52 \pm 3$  K on the same sample. This has been interpreted as an effect of the different time constants of the measurements being  $10^{-2}$  sec. and  $10^{-11}$  sec, respectively.

Our experiments in (Eu,Sr)S also yield a decrease of the measured transition temperature  $T_f$  by increasing the time constant of the measurement (Fig. 15), but it is astonishing that the change in  $T_f$  persists down to very low measuring frequencies. This first observation of the frequency dependence of the ac susceptibility maximum in a spin glass was already mentioned by us in Ref. 14.

Since that time, von Löhneysen *et al.*<sup>27</sup> also reported on a frequency dependence of  $T_f^*$  in the spin-glass samples  $(\text{Gd},\text{La})\text{Al}_2$  with 0.6 and 1 at. % Gd. The experimental situation in 3d-transition-metal spin glasses is not clear: while Zibold<sup>28</sup> concluded that the frequency effect he observed in concentrated AuFe is due to chemical clustering, Dalberg *et al.*<sup>29</sup> did not see any frequency effect in dilute AgMn.

For an understanding of these marked time effects of  $\chi(T_f)$  in (Eu,Sr)S we first try to analyze the data by the simple concept of superparamagnetic clouds.<sup>5</sup> In this phenomenological model one assumes the existence of independent magnetic clusters which can relax between different orientations separated by an energy barrier  $E_a$ . The relaxation time  $\tau$  is described

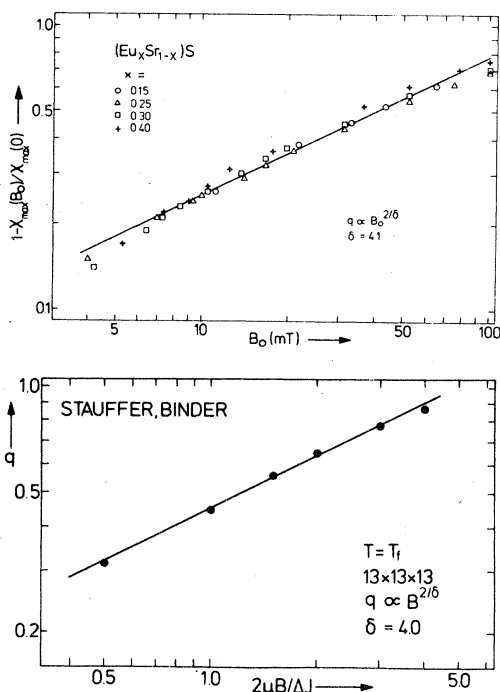


FIG. 17. Depression of  $\chi_{\max}$  as a function of applied field  $B_0$  in (Eu,Sr)S, yielding a critical exponent  $\delta = 4.1$ . Below, the field dependence of the Edwards-Anderson order parameter  $q$  at  $T_f$  in three dimensions, calculated by Stauffer and Binder,<sup>6</sup> also shows  $\delta = 4.0$  ( $B$  in units of  $\Delta J$ , the width of the interaction distribution).

by an Arrhenius law:

$$\tau = \tau_0 \exp(E_a/k_B T), \quad (18)$$

where  $\tau_0$  is some intrinsic time constant. The concept implies that all the clusters with an energy barrier  $E_a$  are blocked at a temperature  $T_B$  for which the measuring time  $\tau_m$  becomes

$$\tau_m = \tau_0 \cdot \exp(E_a/k_B T_B). \quad (19)$$

Hence, the model predicts a dependence of the blocking temperature on the measuring frequency  $\nu$

$$\Delta(T_B)^{-1} = -\frac{k_B}{E_a} \cdot \Delta \ln \nu. \quad (20)$$

One realizes that this simple concept can describe the variation of  $T_f$  with frequency, measured in the ac susceptibility experiments on (Eu,Sr)S (Fig. 15). By comparing the measured dependence [Eq. (4)] with the predicted one [Eq. (20)] one can derive the "mean" anisotropy energy  $E_a$ . The values increase with Eu concentration  $x$  from  $E_a/k_B = 9$  K for  $x = 0.10$  up to  $E_a/k_B = 204$  K for  $x = 0.40$  (see Table I).

In Sec. III E and Fig. 15 we have shown that the  $T_f^{dc}$  values determined from the static susceptibility do not coincide with the  $T_f^{ac\phi}$  values determined by extrapolation of Eq. (20). This demonstrates that the cluster model of Tholence and Tournier contains only part of the truth. An appropriate theoretical concept does not exist up to now.

Our systematic experimental study, however, yields the following concentration dependences which may give some hints for an improvement of the model. The data compiled in Table I exhibit that the difference between the ac- and dc-values of  $T_f$  increases with decreasing Eu concentration

$$(T_f^{ac\phi} - T_f^{dc}) \propto x^{-1}, \quad (21)$$

whereas the difference between two  $T_f^{ac}$  values measured at a constant frequency interval is found to be independent of the concentration  $x$

$$\Delta T_f^{ac} / \Delta \ln \nu = \text{const}. \quad (22)$$

As an example, we observe a temperature difference of 0.10 K by measuring the ac- $\chi$  maximum with frequencies of 4200 and 12 Hz, independent of  $x$  in  $\text{Eu}_x\text{Sr}_{1-x}\text{S}$ . Thus the discrepancy between the ac- and dc-values of  $T_f$  seems to be different in origin from the frequency dependence of  $T_f^{ac}$  as will be discussed below.

### E. Concentration dependences

In this section we consider the observed concentration ( $x$ ) dependences of several properties of

$\text{Eu}_x\text{Sr}_{1-x}\text{S}$ . First of all, our experiments give evidence on the existence of a low-concentration limit of the spin-glass regime in (Eu,Sr)S. Figure 14 shows that the transition temperatures  $T_f$  determined from the dc- and ac- $\chi$  measurements point towards a critical concentration

$$x_p \approx 0.13 \quad (23)$$

for the magnetic behavior of  $\text{Eu}_x\text{Sr}_{1-x}\text{S}$ :  $T_f^{dc}$  extrapolates to zero at this value, and the  $T_f^{ac}$  values exhibit a change in their concentration dependence near  $x_p$ . Such a critical concentration is further supported by Fig. 18: the slope  $S(x)$  defined in Eq. (4) and determined from Fig. 15 changes with  $x$  more slowly below  $x_p$  than above. In addition, the difference and the ratio between the extrapolated  $T_f^{ac\phi}$  value and the measured  $T_f^{dc}$  value increase by magnetic dilution towards  $x_p$ .

It is interesting to stress the coincidence of the experimentally determined critical concentration  $x_p \approx 0.13$  in  $\text{Eu}_x\text{Sr}_{1-x}\text{S}$  with the percolation threshold  $x_p = 0.136$  calculated for an fcc lattice with nearest- and next-nearest-neighbor interactions.<sup>30</sup> Indeed, as pointed out in the Introduction, the exchange interactions in insulating (Eu,Sr)S can be assumed to be predominantly of short range up to the second-nearest neighbors.

Apparently, the magnetic behavior of  $\text{Eu}_x\text{Sr}_{1-x}\text{S}$  changes below  $x_p$ . One striking difference can be observed in Fig. 16 where the temperature dependence

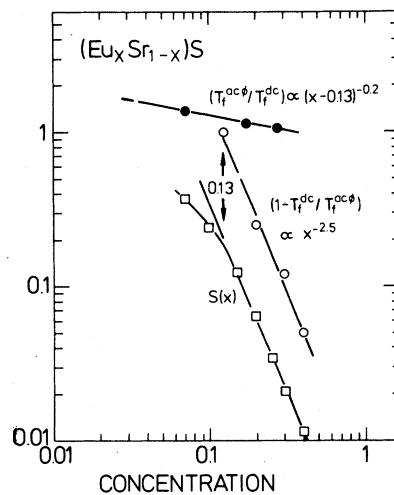


FIG. 18. Concentration dependence of the position of the susceptibility maximum as measured by the dc method  $T_f^{dc}$ , and the ac method  $T_f^{ac}$ , in comparison with the extrapolated values,  $T_f^{ac\phi}$ , as described in the text. Curves are shown for (i) the slope  $S(x)$  of the relation  $(T_f^{ac})^{-1} = -S(x) \cdot \log \nu$ , (ii)  $(1 - T_f^{dc}/T_f^{ac\phi})$  vs  $x$ , and (iii)  $(T_f^{ac\phi}/T_f^{dc})$  vs  $(x - 0.13)$ . The value  $S(x)$  for  $x = 0.07$  is taken from Ref. 31.

of the susceptibility of  $\text{Eu}_{0.10}\text{Sr}_{0.90}\text{S}$  shows a maximum only for the ac measurement, but not for the static measurement with small applied fields. This behavior is markedly different from that of samples with  $0.15 \leq x \leq 0.50$ , where at very low temperatures a decreasing or constant (dependent on the external fields) static susceptibility with decreasing temperature is measured. At low-Eu concentration  $x$ , the dipolar interaction must play a dominant role for the magnetic behavior in  $\text{Eu}_x\text{Sr}_{1-x}\text{S}$ , since it is of the order of 1 K for Eu nearest neighbors. Below the percolation concentration  $x_p$  the blocking of superparamagnetic clusters occurs as a dominant feature caused by intracluster dipolar interactions. As a consequence, remanent magnetizations and their relaxation appear. This has already been reported by Holtzberg *et al.*<sup>22</sup> and has been interpreted in terms of a "dipolar spin glass". In our opinion, however, those properties are not sufficient to characterize a spin glass; they are well-known features in superparamagnetism. A detailed study of the lower limit of the spin-glass regime in (Eu,Sr)S will be published soon.<sup>15</sup> It will be shown that the simple model of superparamagnetism is in good agreement with the experimental results. This is not surprising, since below the percolation threshold  $x_p = 0.13$  in  $\text{Eu}_x\text{Sr}_{1-x}\text{S}$  one really has to deal with isolated magnetic clusters.

With increasing concentrations  $x$  more lattice sites are occupied with Eu atoms. At the critical concentration  $x_p$  an infinite ranged "cluster" appears for the first time. Above  $x_p$  a model considering only isolated clusters is expected to breakdown for a general description of the magnetic behavior. In fact, as outlined in this paper, only some aspects of the experimental results are found to be in agreement with such a cluster concept. A more realistic model also has to take into account the interactions between the magnetic "clouds" in order to explain the spin-glass properties of (Eu,Sr)S.

Above the percolation threshold  $x_p$  the probability for the occupation of magnetic lattice sites formally is high enough to build up a long-range magnetic order. The strong competition between the ferro- ( $J_1$ ) and antiferromagnetic ( $J_2$ ) exchange interactions in (Eu,Sr)S, however, prevents ferro- or antiferromagnetism up to concentrations as high as  $x_c = 0.5$ , as has been proved experimentally.<sup>20</sup> The presence of competing ferro- and antiferromagnetic exchange locally disturbs the correlation between the spin direction and the sign of the interaction, generating "frustrated" interactions. Obviously, one has to assume that above  $x_p$  within the infinite network of exchange interactions, some bonds are present where the negative exchange is strong enough to prevent the system from establishing a ferromagnetic ground state at low temperature. Since there is a random distribution of magnetic atoms, those nonferromagnetic coup-

lings show no periodic structure, and the magnetic properties of  $\text{Eu}_x\text{Sr}_{1-x}\text{S}$  with Eu concentrations  $x$  between 0.13 and 0.5 proved to be spin glass like in the present work.

However, one has to strictly distinguish between superparamagnetism and spin-glass behavior. A realistic theory, not available up to now, has to explain for instance the measured frequency dependence of the critical temperature  $T_f^{sc}$ : the variation  $\Delta T_f^{sc}/\Delta \ln \nu$  is independent of concentration  $x$  in the spin-glass regime (above  $x_p$ ), which is found here [Eq. (22)], whereas below  $x_p$  Tholence *et al.*<sup>31</sup> observed  $\Delta T_f^{sc}/\Delta \ln \nu$  to vary linearly with  $x$ . The difference measured between  $T_f^{sc}$  and  $T_f^{dc}$ , being more pronounced at lower concentrations [Eq. (21)], appears as a hint on the relevant interaction *between* the stronger magnetically coupled regions. It seems reasonable that the negative exchange interactions can break up the infinite network and prevent it to show long-range ferromagnetism more easily at lower concentrations, so that such time effects grow with decreasing  $x$ . On the other hand, with increasing  $x$  the regions with short-range coupling grow, due to the increasing tendency towards ferromagnetism, and field effects become stronger as discussed in Sec. IV C. A quantitative explanation of the high critical concentration for the spin-glass-to-ferromagnetism transition in (Eu,Sr)S is now worked out by Binder and Kinzel.<sup>32</sup>

## V. CONCLUSIONS

With the aid of a systematic study of low-field magnetization, ac susceptibility, and neutron diffraction on the insulating system  $\text{Eu}_x\text{Sr}_{1-x}\text{S}$ , we obtained experimental evidence on the spin-glass behavior of the samples with concentrations  $0.13 \leq x \leq 0.5$  at low temperatures. Below the freezing temperature  $T_f$  irreversible magnetic properties were observed (TRM, IRM, time dependence), as in metallic spin glasses, and these varied with the magnetic history of the specimen, i.e., whether or not the sample was cooled through  $T_f$  in an external field. Unusually large field and time effects on the susceptibility maximum were measured in the vicinity of  $T_f$  in (Eu,Sr)S. They were discussed especially with respect to their concentration dependence. A low-concentration limit of the spin-glass regime of  $\text{Eu}_x\text{Sr}_{1-x}\text{S}$  was found experimentally ( $x_p \approx 0.13$ ), which coincides with the percolation threshold of the exchange interactions.

Throughout the paper, a comparison is drawn between the observed behavior in (Eu,Sr)S and that of a metallic spin glass with the aim to learn more in general about random magnetic systems and their ordering. No feature is detected which might give arguments for the existence of different classes of real spin glasses with respect to their metallic or insulating

nature, as Mydosh<sup>9</sup> has claimed recently. Even the outstanding frequency dependence of the susceptibility maximum as observed here was recently measured in the metallic spin glass (Gd, La)Al<sub>2</sub>, too.<sup>27</sup>

The relevant features of the underlying interactions in the nonmetallic (Eu,Sr)S samples were discussed. Obviously, the competition of ferro- and antiferromagnetic exchange, predominantly of short range in insulating (Eu,Sr)S, causes similar properties as the long-range, oscillating RKKY interaction in alloys like AuFe.

We conclude from our systematic data that several properties of (Eu,Sr)S which are more pronounced than in canonical spin glasses with 3d-transition metals can be explained qualitatively by a time effect and thus are eventually connected in origin with the frequency dependence of  $T_f$ : (i) the saturated remanent magnetization  $\sigma_{RM}^{sat}$  is considerably reduced compared to the maximum of the thermoremanent magnetization [Eq. (2)], (ii) the thermal variation of  $\sigma_{RM}^{sat}$  deviates from an exponential decrease at very low temperatures, (iii) the remanent magnetization decays more rapidly, especially at the beginning. It may be that these pronounced features can be traced back to the weak interactions between the 4f-moments in (Eu,Sr)S. As a measure, the ratio  $T_f/x$  was found to be 5 and 26 K,<sup>24</sup> in (Eu,Sr)S and in (Gd,Lu)Al<sub>2</sub>, respectively, as compared to 1000 K in the canonical spin-glass AuFe (with the strong couplings between the 3d-moments).

In an attempt to describe the measured frequency dependence of  $T_f$  with the phenomenological model of superparamagnetic "clouds" proposed by Tholence and Tournier,<sup>5</sup> we have demonstrated that this concept contains only part of the truth. A more realistic model should also take into account the interactions between the magnetic clouds in order to explain the properties of (Eu,Sr)S within the spin-glass regime.

Furthermore, our experiments revealed a drastic change in the magnetic behavior of Eu<sub>x</sub>Sr<sub>1-x</sub>S near  $x_p = 0.13$  which coincides with the calculated percolation threshold of the exchange interactions. Only below  $x_p$  can the frequency dependence of  $T_f$  be successfully explained by the concept of isolated superparamagnetic clusters (as will be reported in detail in Ref. 15). Clearly, the experimental results of (Eu,Sr)S suggest that one has to distinguish between

superparamagnetism and spin-glass behavior.

Finally, concerning the nature of the spin-glass transition at  $T_f$  it remains to be explained theoretically that the change of  $T_f$  observed in (Eu,Sr)S persists down to very low measuring frequencies. Does such an effect support evidence on a nonequilibrium phenomenon at  $T_f$ ? Recently, Monte Carlo simulations of an Ising spin glass by Stauffer and Binder<sup>6</sup> have shown that the anomalously slow relaxation, also observed in the computer simulations, can be traced back to the high ground-state degeneracy, and cannot be maintained as a firm evidence against a phase transition at  $T_f$  in Ising spin glasses.

The situation in Heisenberg spin glasses in three dimensions is even less clear, concerning the computer experiments near  $T_f$ .<sup>33</sup> As mentioned in the Introduction, however, the (Eu,Sr)S spin glass is probably an ideal example of a Heisenberg spin glass. Krey<sup>34</sup> has pointed out that there should be no phase transition for a Heisenberg spin glass below four dimensions. Anderson and Pond<sup>35</sup> have given arguments that for vector spin glasses the three dimensions are the lower critical dimensionality, resulting possibly in the peculiar behavior of real spin-glass samples. The question about the nature of the spin-glass state remains a fascinating problem, and further studies will be worthwhile.

#### ACKNOWLEDGMENTS

One of the authors (H.M.) is indebted to the Centre de Recherches sur les Très Basses Températures (CNRS) Laboratory, Grenoble, for the possibility to perform the static magnetization measurements at very low temperatures during a stay there. The neutron-diffraction experiments have been performed on the D1B multicounter instrument of the ILL reactor in Grenoble. We thank Dr. H. Pink, Siemens AG, München, for the preparation of the samples. It is a pleasure to acknowledge the permanent interest of Professor W. Zinn in this work, many fruitful comments of Professor K. Binder and the continuous support by Professor G. v. Minnigerode. This work is part of the research program of the SFB 125 Aachen-Jülich-Köln. Parts of it have been supported by SFB 126 Göttingen-Clausthal.

<sup>1</sup>J. A. Mydosh, in *Proceedings of the Second International Symposium on Amorphous Magnetism, Troy, 1976*, edited by R. A. Levy and R. Hasegawa (Plenum, New York 1977).

<sup>2</sup>K. Binder, in *Festkörperprobleme (Advances in Solid State Physics)*, edited by J. Treusch (Vieweg, Braunschweig,

1977), Vol. XVII, p. 55.

<sup>3</sup>M. A. Ruderman and C. Kittel, *Phys. Rev.* **96**, 99 (1954).

T. Kasuya, *Progr. Theor. Phys.* **16**, 45 (1956). K. Yosida, *Phys. Rev.* **106**, 893 (1957).

<sup>4</sup>V. Cannella and J. A. Mydosh, *Phys. Rev. B* **6**, 4220 (1972).

- <sup>5</sup>J. L. Tholence and R. Tournier, *J. Phys. (Paris)* **35**, C4-229 (1974).
- <sup>6</sup>D. Stauffer and K. Binder, *Z. Phys. B* **30**, 313 (1978).
- <sup>7</sup>S. F. Edwards and P. W. Anderson, *J. Phys. F* **5**, 965 (1975).
- <sup>8</sup>K. Binder and K. Schröder, *Phys. Rev. B* **14**, 2142 (1976).
- <sup>9</sup>J. A. Mydosh, *J. Magn. Magn. Mater.* **7**, 237 (1978).
- <sup>10</sup>H. Maletta and G. Crecelius, *J. Phys. (Paris)* **37**, C6-645 (1976).
- <sup>11</sup>W. Zinn, *J. Magn. Magn. Mater.* **3**, 23 (1976).
- <sup>12</sup>T. Kasuya, *IBM J. Res. Dev.* **14**, 214 (1970).
- <sup>13</sup>U. Köbler, H. Maletta, and P. Pink (unpublished).
- <sup>14</sup>H. Maletta, W. Felsch, and J. L. Tholence, *J. Magn. Magn. Mater.* **9**, 41 (1978).
- <sup>15</sup>G. Eiselt, J. Kötzler, H. Maletta, D. Stauffer, and K. Binder, *Phys. Rev. B* **19**, (1979).
- <sup>16</sup>G. Toulouse, *Commun. Phys.* **2**, 115 (1977).
- <sup>17</sup>S. Kirkpatrick, *Phys. Rev. B* **16**, 4630 (1977).
- <sup>18</sup>W. Kinzel and K. H. Fischer, *J. Phys. F* **7**, 2163 (1977).
- <sup>19</sup>J. L. Tholence, Ph.D. thesis (Grenoble, 1973)(unpublished).
- <sup>20</sup>H. Maletta and P. Convert, *Phys. Rev. Lett.* **42**, 108 (1979).
- <sup>21</sup>W. Kinzel, *J. Phys. (Paris)* **39**, C6-905 (1978); and unpublished.
- <sup>22</sup>F. Holtzberg, J. L. Tholence, and R. Tournier, in *Proceedings of the Second International Symposium on Amorphous Magnetism, Troy, 1976*, edited by R. A. Levy and R. Hasegawa (Plenum, New York 1977), p. 155.
- <sup>23</sup>C. N. Guy, *J. Phys. F* **7**, 1505 (1977).
- <sup>24</sup>H. v. Löhneysen, J. L. Tholence, and F. Steglich, *Z. Phys. B* **29**, 319 (1978).
- <sup>25</sup>J. Chalupa, *Solid State Commun.* **24**, 429 (1977).
- <sup>26</sup>A. P. Murani and J. L. Tholence, *Solid State Commun.* **22**, 25 (1977).
- <sup>27</sup>H. v. Löhneysen, J. L. Tholence, and R. Tournier, *J. Phys. (Paris)* **39**, C6-922 (1978).
- <sup>28</sup>G. Zibold, *J. Phys. F* **8**, L229 (1978).
- <sup>29</sup>E. D. Dahlberg, M. Hardiman, R. Orbach, and J. Souletie (unpublished).
- <sup>30</sup>N. W. Dalton, C. Domb, and M. F. Sykes, *Proc. Phys. Soc. London* **83**, 496 (1964).
- <sup>31</sup>J. L. Tholence, F. Holtzberg, H. Godfrin, and H. v. Löhneysen, and R. Tournier, *J. Phys. (Paris)* **39**, C6-928 (1978).
- <sup>32</sup>K. Binder and W. Kinzel (unpublished).
- <sup>33</sup>K. Binder, *Z. Phys. B* **26**, 339 (1977).
- <sup>34</sup>U. Krey, *Phys. Lett. A* **64**, 125 (1977).
- <sup>35</sup>P. W. Anderson and C. M. Pond, *Phys. Rev. Lett.* **40**, 903 (1978).